Est. 1984

**ORIENTAL JOURNAL OF CHEMISTRY**
An International Open Free Access, Peer Reviewed Research Journal

www.orientjchem.org

ISSN: 0970-020 X
CODEN: OJCHEG
2016, Vol. 32, No. (5):
Pg. 2633-2639

# Effect of $CO_2$ on the Conversion of Isobutane Over Iron, Cerium and Molybdenum Mixed Oxides

**DAIFALLAH AL-DHAYAN, SAAD AL-KAHTANI and AHMED AOUISSI***

Chemistry Departement, College of Science, King Saud University. Riyadh. Kingdom of Saudi Arabia.
*Corresponding author E-mail : aouissed@yahoo.fr

http://dx.doi.org/10.13005/ojc/320535

(Received: September 26, 2016; Accepted: October 14, 2016)

**ABSTRACT**

A series of cerium and iron mixed oxide catalysts were prepared by thermal decomposition of $Fe_{1.5}PMo_{12}O_{40}$ and $Ce_{1.5}PMo_{12}O_{40}$ heteropolyanions mixture. The prepared catalysts have been characterized and tested for the conversion of isobutane in the presence of $CO_2$. Characterization by XRD showed that besides $Fe_2O_3$ and $CeO_2$, $\alpha$-$MoO_3$ was the main phase formed after thermal treatment. The effect of the support, the reaction temperature, and the presence of $H_2O$ in the reactant mixture was investigated. It has been found that the support enhanced both the conversion and isobutene selectivity. As for the reaction temperature and addition of water, it has been found that increasing the temperature increased both the conversion and isobutene selectivity, whereas the presence of water increased the isobutene selectivity but decreased the conversion.

**Keywords:** Isobutene, Isobutene, Polyoxometalates, Mixed oxides, Carbon dioxide.

## INTRODUCTION

Isobutene is one of the most important chemical intermediates used in the production of a variety of products, including the high-octane fuel. The increasing demand for isobutene has drawn considerable attention towards enhancing its production. Currently, it is produced industrially by the dehydrogenation of isobutane (IB) over $Cr_2O_3$-$Al_2O_3$ catalyst at 627°C [1]. Owing to the endothermic nature of this reaction, elevated temperatures are necessary to achieve acceptable levels of conversion. These extreme operating conditions favor coke formation and catalyst deactivation. Furthermore, the formation of carbon oxides is thermodynamically more favorable than the formation of Isobutene. Consequently, the selectivity of Isobutene decreases with the increase of IB conversion when oxygen is used as an oxidizing agent[2,3]. Therefore, much attention has been devoted to develop a new catalyst to make Isobutene production more economical and environmentally friendly. For this reason, several investigations have been carried out on the dehydrogenation of IB in the presence of $CO_2$[4,6]. This reaction is attractive because carbon dioxide is naturally abundant and the resulting process would lead to consumption of a greenhouse gas. However, the Isobutene yield and catalyst stability still major

drawbacks for practical applications. Here we report the conversion of IB in the presence of CO2 in gas phase over cerium-iron-molybdenum mixed oxides prepared by thermal decomposition of $Ce_{1.5}PMo_{12}O_{40}$ and $Fe_{1.5}PMo_{12}O_{40}$ as heteropolyanion precursors. The effect of the support ($Al_2O_3$), cerium molar ratio, reaction temperature, catalyst weight and addition of water on IB conversion was investigated.

## EXPERIMENTAL

### Preparation of the catalysts

The heteropolyanion precursors, $Fe_{1.5}PMo_{12}O_{40}$, $Ce_{1.5}PMo_{12}O_{40}$ used for the preparation of the unsupported and alumina suported mixed oxides catalysts were prepared according to a now well-known method [7]. A series of iron-cerium-molybdenum mixed oxides supported on 70% (by weight) of alumina having various Ce/Fe molar ratios have been prepared by incipient-wetness impregnation of $Al_2O_3$ with aqueous solutions of $Fe_{1.5}PMo_{12}O_{40}$ and $Ce_{1.5}PMo_{12}O_{40}$ in desired volume ratios. The resulting mixture was maintained at about 50°C until dryness evaporation, dried at 100°C for several hours and calcined at 700°C under an air flow of 6 L/h for 2 h. The prepared catalysts are denoted Ce-Fe-Mo-x where x is the Ce/(Ce+Fe) molar ratio : Ce-Fe-Mo-0; Ce-Fe-Mo-0.33; Ce-Fe-Mo-0.50; Ce-Fe-Mo-0.67.

### Characterization of the catalysts

The Keggin structure of the heteropolyanion precursors and the mixed oxides obtained by thermal treatment of the samples was checked by FT-IR. FT-IR spectra were recorded with an infrared spectrometer GENESIS II-FTIR (4000-400 $cm^{-1}$) as KBr pellets. The Powder X-ray diffraction (XRD) patterns were recorded on Siemens D5000 diffractometer with Cu-$K_\alpha$ (I = 1.5418Å) radiation using Cu Ka radiation.

### Catalytic measurements

Catalytic tests were carried out under atmospheric pressure using a fixed-bed continuous-flow reactor made of a Pyrex tube. The catalytic charge packed in a stainless reactor, was activated by $CO_2$ flow for 2 h at the reaction temperature. After activation, the reagent mixture $CO_2$ / IB with the desired molar ratio at a flow rate of 50 ml $min.^{-1}$ was admitted in the reactor. The flow of $CO_2$ and IB gas were controlled by mass flow controller. The products of the reaction were analyzed with a gas

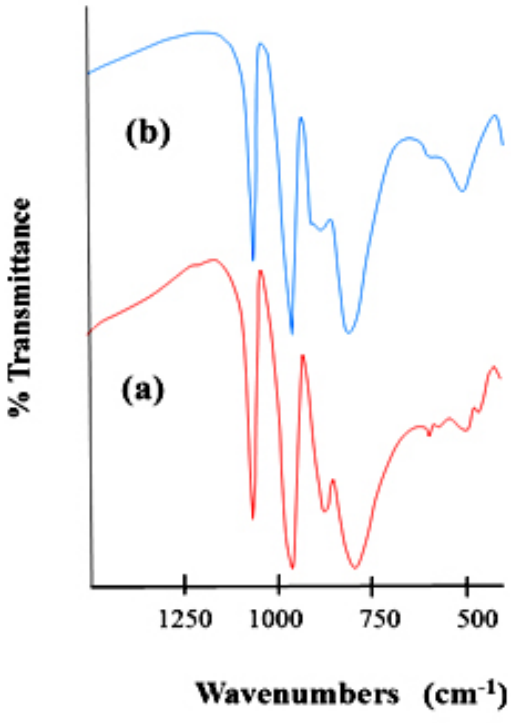


**Fig. 1: FTIR spectra of the heteropolyanions precursors. (a) $Fe_{1.5}PMo_{12}O_{40}$ (b) $Ce_{1.5}PMo_{12}O_{40}$**

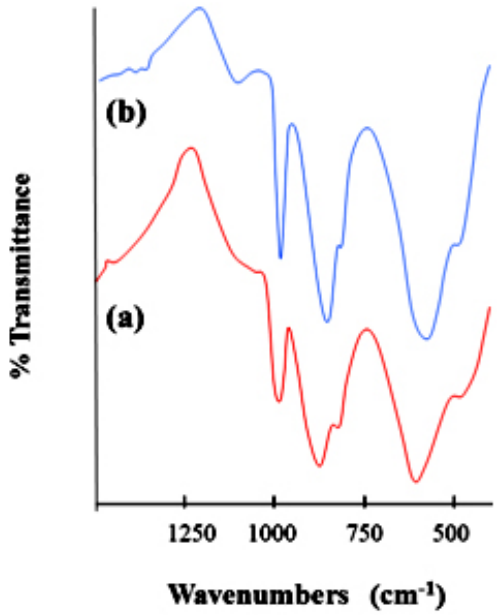


**Fig. 2: FTIR spectra of the mixed oxides (a) Fe-Mo-oxides (b) Ce-Mo-oxides**

phase chromatograph type Agilent 6890 N equipped with a flame ionization detector (FID), a thermal conductivity detector (TCD) and a capillary column (HP-PLOT Q length 30 m ID 0.53 mm).

## RESULTS AND DISCUSSION

### FTIR characterizations

FTIR spectra of the Keggin-type heteropolyanion precursors, $Fe_{1.5}PMo_{12}O_{40}$, $Ce_{1.5}PMo_{12}O_{40}$ used for the synthesis of oxide catalysts are shown in Figure 1. The main characteristic features of the Keggin structure are observed for both catalysts. The four bands characteristic of the kegging structure observed at 1080–1060, 990–960, 900–870, and 810–760 $cm^{-1}$ are assigned to the asymmetric stretching vibrations of the $\gamma_{as}$(P–Oa), $\gamma_{as}$ (Mo–Od), $\gamma_{as}$ (Mo–Oc–Mo), and $\gamma_{as}$ (Mo–OC–Mo) bonds, respectively[8, 9]. The FTIR spectra of the oxide catalysts obtained by thermal treatment at 700°C are shown in Figure 2. It can be seen that after thermal treatment the typical bonds of the Keggin structure disappeared and replaced by characteristic bonds of Mo-oxo species closely resembling the orthorhombic molybdenum trioxide, referred to as $\alpha$-$MoO_3$.

### XRD measurements

The XRD patterns of the obtained iron molybdenium mixed oxides (denoted as Fe-Mo-oxides) and cerium molybdenium mixed oxides (denoted as Ce-Mo-oxides) are shown in Figure 3 and presented in Table 1. Table 1 presents the d-spacings that correspond to the most significant peaks in the patterns of the mixed oxides Fe-Mo and Ce-Mo and the orthorhombic $\alpha$-$MoO_3$ oxide[10]. These results showed that besides the iron and cerium oxides resulting from the corresponding cation (Fe and Ce, in the precursor heteropolyanions, the mixed oxides contain $\alpha$-$MoO_3$ as main phase. The diffraction peaks observed at 3.006 Å, 2.702 Å, and 1.632 Å which are ascribed to (111), (200), (220) crystal planes are characteristic of the cubic $CeO_2$ (JCPDS Card No. 43-1002) [11]. The reflections observed with d spacing at 3.44 Å, 3.25 Å, 3.07 Å, and 2.69 Å (JCPDS No. 30-0304) are characteristics of $Ce_2Mo_4O_{15}$. The indexed XRD patterns for the iron oxides showed that the Mo-Fe catalyst contains peaks of rhombohedral $\alpha$-$Fe_2O_3$ at d-values 2.67, 1.44, (matched with PDF No-01-079-007) and the orthorhombic ferric molybdate (Fe-$MoO_3$)[12]. For both iron and cerium mixed oxides, other phases could be present as traces. It is worth noting that for several oxides the coexistence of various phases besides the main phase has been observed [13, 14].

### Catalytic activity

The mixed oxide Ce-Fe-Mo-0.67 prepared by chemical and mechanical mixing have been tested in the conversion of IB. The variation of the IB conversion as a function of time on stream is shown in Figure 4. It can be seen from these results that both catalysts have the same catalytic properties. Indeed, we notice that both catalysts led to the same values of conversion and the same stability during the reaction time. It is also noted that they led to the same selectivities of the products (Figure 5). It is worth noting that for each of the catalysts, the selectivity in isobutene decreases with time in favor of the selectivity of cracking products.

### Effect of Support

Figure 6 showed the IB conversion and product selectivites obtained over unsupported Fe-Ce-Mo catalyst and Alumina supported Fe-Ce-Mo. The obtained conversion and isobutene selectivity were 5.54% and 26.9% respectively whereas those obtained over the alumina supported catalyst are

**Table 1: Interplanar Spacings *dhkl* (A°) and Relative Intensities of Orthorhombic $\alpha$-$MoO_3$ (Ref. 15): Comparison with the XRD Patterns of Fe-Mo-oxides and Ce-Mo-oxides**

| | d-spacings (A°) | |
|---|---|---|
| $\alpha$-$MoO_3$ | Mo-Fe | Mo-Ce |
| 6.942 | 7.070 | 6.901 |
| 3.810 | 4.585 | 4.114 |
| 3.462 | 3.835 | 3.807 |
| 3.260 | 3.501 | 3.464 |
| 2.653 | 3.280 | 3.260 |
| 2.308 | 3.018 | 3.006 |
| | 2.670 | 2.881 |
| | 2.555 | 2.702 |
| | 1.452 | 2.143 |
| | 1.437 | 1.988 |
| | | 1.579 |
| | | 1.482 |
| | | 1.449 |

(5.79%) and selectivity (28.8%) respectively. These results indicated that the alumina support has slightly improved the catalyst performance. This result indicated that the oxidative dehydrogenation leading to the isobutene formation required the presence of Lewis acid sites.

**Effect of Ce/Fe ratio**

The series of alumina supported Fe-Ce-Mo-x catalysts were tested for the conversion of IB. The dependence of the conversion and the product selectivities on Cerium molar ratio at the steady state are reported in Figure 7. The results showed that the highest conversion of IB (5.8%) and the highest selectivity of isobutene (28.8%) were obtained over Fe-Ce-Mo-0.67 catalyst. In contrast the lowest conversion (4.7%) and the highest selectivity of isobutene (21.2%) were obtained over Fe-Ce-Mo-0.50 catalyst. Since the Fe-Ce-Mo-0.67 catalyst was the best catalyst, it was selected for further

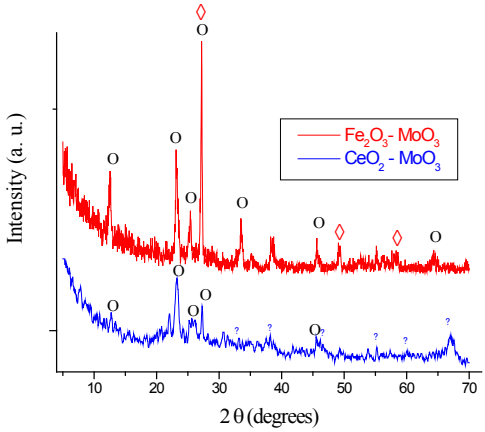


**Fig. 3: XRD patterns of (a) iron-molybdenum mixed oxides and cerium-molybdenum mixed oxides (b) where o denotes reflection of $MoO_3$, ◊ denotes reflection of $Fe_2O_3$, n denotes reflection of $CeO_2$.**

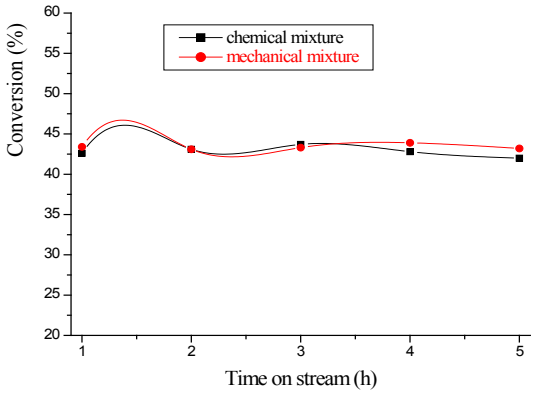


**Fig. 4: Dependence of the conversion on time on stream for the conversion of IB catalyzed by Ce-Fe-Mo-0.67 prepared by chemical and mechanical mixing**

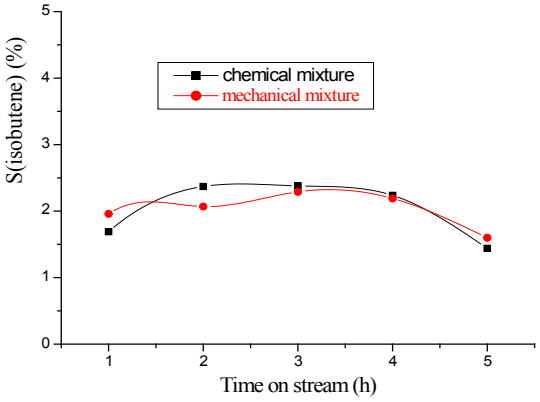


**Fig. 5: Dependence of the isobutene selectivity on time on stream for the conversion of IB catalyzed by Ce-Fe-Mo-0.67 prepared by chemical and mechanical mixing**

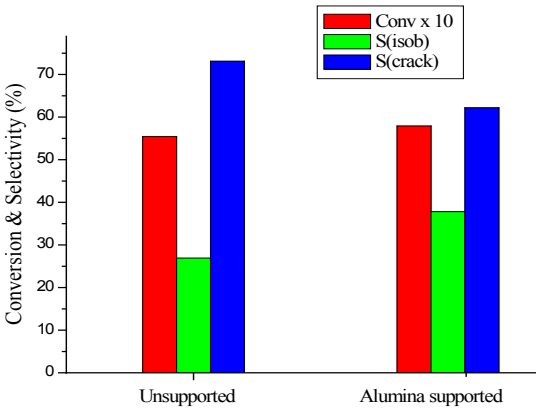


**Fig. 6: Conversion of IB and product selectivities obtained over the unsupported and alumina supported catalyst. Reaction conditions: reactions temperature 600°C, catalyst amount 0.1g and n($CO_2$)/n( isobutene) = 5**

investigations such as the effect of the catalyst amount, reaction temperature and addition of water on the IB conversion.

**Effect of the catalyst amount**

The variation of the conversion and selectivities as a function of the mass of the catalyst is depicted in Figure 8. It can be seen from the figure that both the conversion of IB and the selectivity of isobutene increased with the increase of the mass of the catalyst. Indeed the conversion increased from 5.8% to 7.5% and the selectivity of isobutene increased from 28.8% to 39.9% when the mass of the catalyst was increased from 0.1g to 0.9 g. In contrast the selectivity of cracking products decreased with the increase of the mass of the catalyst. This result can be explained by the fact that at higher catalyst mass the residence time is long which allow to the dehydrogenation reaction to occur whereas at lower catalyst mass, the residence time is short which decrease the probability for the dehydrogenation

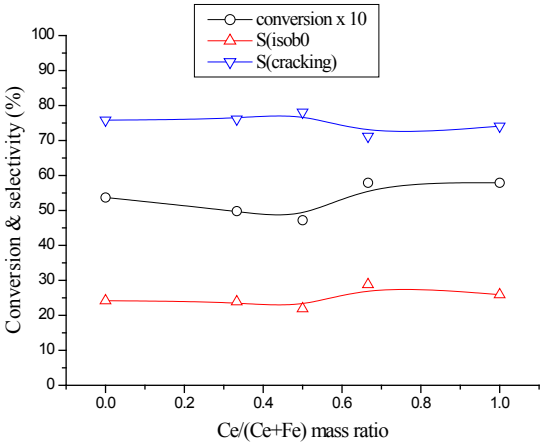


**Fig. 7: Conversion of IB and selectivity to isobutene and cracking products at the steady state as a function of Ce/(Ce+Fe) molar ratio. Reaction conditions: reaction temperature 600°C, catalyst amount 0.1g, n($CO_2$)/n ( isobutene) = 5**

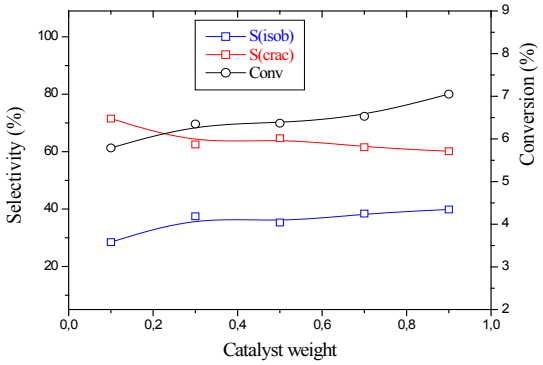


**Fig. 8: Conversion of IB and product selectivities as a function of Ce/(Ce+Fe) molar ratio. Reaction conditions: reaction temperature 600°C, n($CO_2$)/n( IB) = 5**

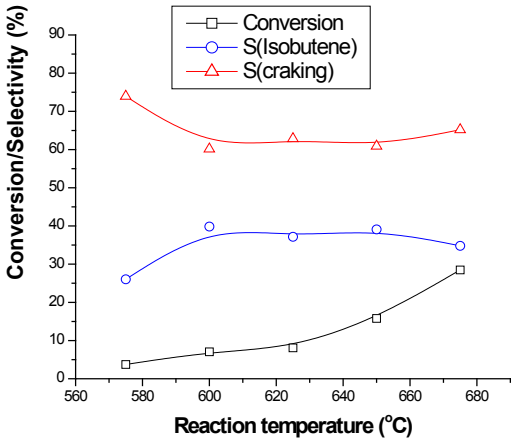


**Fig. 9: Conversion of IB and product selectivities as a function of reaction temperature. Reaction conditions: catalyst amount 0.1g, feed composition: n($CO_2$)/ n(isobutane) = 5**

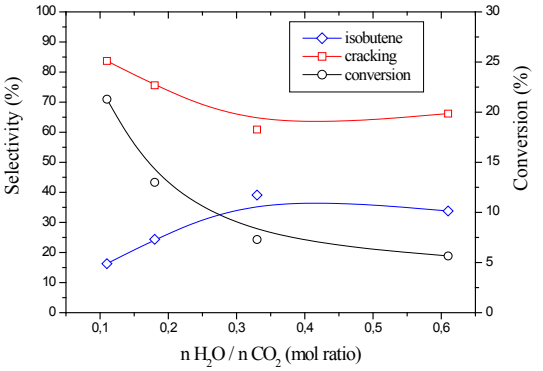


**Fig. 10: Conversion of IB and selectivity to isobutene and cracking products as a function of $CO_2$/$H_2O$ molar ratio**

reaction to occur and thermal cracking reactions occur.

**Effect of reaction temperature**

The Figure 9 shows the dependence of the IB conversion and the product selectivities on the reaction temperature. As expected the conversion increased with increasing the temperature. As for the selectivity, the results showed that the isobutene selectivity increased with the temperature whereas that of cracking products decreased. The isobutene selectivity increased from 26.0% to 39.7% when the temperature increased from (575°C) to (600°C). Beyond 600°C, the selectivity of both isobutene and cracking products remained almost stable whereas the conversion still increasing. This result can be explained by the fact that at higher temperatures, $CO_2$ removes the carbon deposited (responsible of the catalyst deactivation) from the catalyst surface. In fact, it has been reported that the regeneration of deactivated $Ni/L_{a2}O_3$ and $Ni/Y_2O_3$ catalysts was due to the partial removal of carbon deposits through CO formation (reverse Boudouard reaction)[15-19]. The increase of the selectivity of isobutene form 575 °C to 600°C is in agreement with those reported in the literature[20] where it has been mentioned that the temperature for the carbon dioxide to be activated over VMgOx catalyst was around 527–553°C. $CO_2$ enhanced the yield of IB dehydrogenation significantly. In the opinion of the authors, $CO_2$ as a weak oxidant can eliminate hydrogen produced during the dehydrogenation through the reverse water gas shift (RWGS) reaction [21-23]:

$$C_4H_{10} \longrightarrow C_4H_8 + H_2$$
$$CO_2 + H_2 \longrightarrow CO + H_2O$$

**Effect of addition of water**

The effect of water introduction as reactant besides $CO_2$ on IB conversion was also investigated. The reactions were carried out at 600°C over Fe-Ce-Mo-0.67 catalyst with a reactant mixture *n*(CO2)/*n*(IB) = 3. The dependence of the conversion and the product selectivities on water proportion is presented in Figure 10. The results showed that the addition of water decreased both the conversion and cracking products but increased the isobutene selectivity. Indeed, when the ($nH_2O/n\ CO_2$) ratio increased from 0.1 to 0.61, the conversion decreased from 5.66% to 21.3% whereas the isobutene selectivity increased form 16.3% to 33.8% to. This result indicated that the presence of water in the reactant mixture favors the oxidative dehydrogenation of IB leading to the formation of isobutene, whereas $CO_2$ favors the formation of the cracking products.

## CONCLUSION

Iron, cerium and molybdenum mixed oxides catalysts prepared by thermal treatment of Keggin-type heteropolymolybdates as precursors were characterized and tested for the conversion of IB in the presence of $CO_2$.

Characterization of the catalysts by XRD showed that besides iron and cerium oxides the catalysts contain á-$MoO_3$ as main phase.

The effects of various parameters such as the support ($Al_2O_3$), the catalyst weight, the reaction temperature and the presence of water in reactant mixture were investigated. It has been found that $Al_2O_3$ improved both the conversion and isobutene selectivity which indicated that the oxidative dehydrogenation leading to the isobutene formation required the presence of Lewis acid sites.

IB reaction over different amounts of showed that both the conversion of IB and selectivity of isobutene increased with increasing the mass of the catalyst.

The dependence of the IB conversion on the temperature showed that beyond 600°C, $CO_2$ enhanced the yield of IB dehydrogenation significantly.

The presence of water in the reactant mixture favors the oxidative dehydrogenation of IB leading to the formation of isobutene, whereas $CO_2$ favors the formation of the cracking products.

## ACKNOWLEDGMENT

The Authors extend their appreciation to the Deanship of Scientific Research at King Saud University for funding the work through the research group project No RGP-VPP-025

## REFERENCES


1. Matsuda, T.; Koike, I.; Kubo, N.; Kikuchi, E. *Appl Catal A*. **1993**, *96*, 3-13
2. Al-zahrani, S. M.; Elbashir, N O.; Abasaeed, A. E.; Abdulwahed M. *J Mol Catal A*. **2004**, *218*, 179-186
3. Li, L.; Yan, Z F. *Progr Chem*. **2005**, *17*, 651-659
4. Dias.; C. R.; Zavoianu, R.; Portela, M. F. *Catal Commun*. **2002**, *3*, 85-90
5. Bi, Y. L.; Zhen, K. J.; Valenzuela, R. X.; Jia, M. J.; Corberán V. C. *Catal Today*. **2000**, *61*, 369-375
6. Ogonowski, J.; Skrzñska, E. *Catal Lett*. **2006**, *111*, 79-85
7. Aouissi, A.; Apblett, A. W.; AL-Othman, Z. A.; Al-Amro, A. *Transition Met Chem*. **2010**, *35*, 927-931.
8. Rocchiccioli-Deltcheff, C.; Fournier, M.; Franck, R.; Thouvenot, R. *Inorg. Chem.* **1983**, *22*, 207-216
9. Rocchiccioli-Deltcheff, C.; Fournier, M. *J. Chem. Soc. Faraday Trans*. **1991**, *87*, 3913-3920
10. Andersson, G.; Magnéli, A. *Acta Chem. Scand*. **1950**, *4*,793-797
11. Huang, S.; Liu, S.; Zhu, Q.; Zhu, X.; Xin,W.; Liu, H.; Feng, Z.; Li, C.; Xie, S.; Wang, Q.; Xu, L. *Appl Catal A*. **2007**, *323*, 94-103
12. Massarotti, V.; Flor, G.; Marini, A. *J Appl Cryst*. **1981, *14***, p. 64-65
13. Carriazo, J. G.; Molina, R.; Moreno, S. *Appl Catal A*. **2008**, *334,* 168-172
14. Rashad, M. M. *Mater Sci Eng B*. **2006,** *127*, 123-129
15. Bednarczuk, L.; Ramírez de la Piscina, P.; Homs, N. *Int. J. Hydrogen Energy*. **2015**, *40*, 5256-5263
16. Jiang, N.; Burri, A.; Park, S. E. *Chinese Journal of Catalysis*. 2016, *37*, 3–15
17. Irun, O.; Sadosche, S. A.; Lasobras, J.; Soler, J.; Frances, E.; Herguido, J.; Menendez, M. *Catal. Today*, **2013**, *203*, 53-59.
18. Hong, D.Y.; Vislovskiy, V. P.; Hwang, Y. K.; Jhung, S. H.; Chang, J. S. *Catal. Today*, **2008**, *131*, 140-145.
19. Burri, A.; Jiang, N.; Yahyaoui, K.; Park, S. E. *Appl. Catal. A*. **2015**, *495*, 192-199.
20. Ogonowski, J.; Skrzyñska, E. *Catal Commun*. **2009**, *11*, 132-136
21. Ding, J. F.; Qin Z. F.; Li X. K.; Wang G. F.; Wang J. G.; *J Mol Catal A*. **2010**, *315*, 221-225
22. Shimada, H.; Akazawa, T.; Ikenaga, N.; Suzuki, T. *Appl Catal A*. **1998**, *168*, 243-250
23. Sun, A. L.; Qin, Z. F.; Chen, S. W.; Wang, J. G. *J Mol Catal A*. **2004**, *210*, 189-195
24. Ping, H.; Kou, Z.; Xu, G.; Wu, S. *J. Environmental Chemical Engineering*. **2016**, *4*, 3253–3259